Modelling of thermoforming processes for bio-degradable thermoplastic materials

M. K. Warby and J. R. Whiteman

Abstract Thin walled container structures have for decades been manufactured from oil based polymeric materials using thermoforming processes. Since the 1980's computational modelling has been used to simulate and aid in the development of these processes. Oil based materials are not eco-friendly, as they do not degrade after use and cause problems of waste. We report here on the computational modelling, using solid mechanics and elasto-plastic deformation, of the thermoforming of food packaging structures made from starch based (bio-degradable) biomaterials. It is shown that, with limited data, it is possible to predict satisfactorily the wall thickness of thermoformed structures. This work was undertaken in BICOM in collaboration with engineering colleagues at Brunel University London, and in association with companies from the polymer industry to provide technical information for their customers.

1 Introduction and Background

Many thin-walled food packaging structures are made using thermoforming processes in which hot thin oil-based polymer sheets are forced under pressure into moulds, and then cooled. These structures, being made of oil based polymers, are not eco-friendly as they do not degrade after use. Unless they are recycled, which is difficult, these structures exist long term causing worldwide waste problems. To address this, manufacturers are increasingly turning to bio-degradable bio-materials (thermoplastics) for their thermoforming for packaging. A family of such starch based bio-materials now being used increasingly for packaging is based on maize. However, these materials are relatively new and not well understood. This project aimed at finding appropriate constitutive models for the computational modelling of the deformation of the thermoplastic material Plantic$^{®}$. Necessary temperature and humidity controlled experimentation to determine the material properties of Plantic$^{®}$, and the wall thicknesses of some thermoformed structures, was performed by our collaborators Professor J Song and Dr D Szegda of the Dept of Mechanical Engineering at Brunel University London. This experimentation, on which we report in Section 2, led us to adopt an elasto-plastic

M.K. Warby and J. R. Whiteman are in BICOM, Department of Mathematics, CEDPS, Brunel University London UB8 3PH.

model for the deformation. Section 3 describes the mathematical and computational modelling, including the simplifying assumptions that have been made, and we discuss briefly some features of the finite element model that was implemented using the commercial software LS-DYNA, see [2]. Results of the modelling are shown in Section 4. These demonstrate that the wall thickness distribution of a thermo-formed starch structure can be predicted quite well, in spite of limited data availability.

2 Remarks on material testing

Many experimental tests were performed by Szegda, see [3, chap. 3], on the thermoplastic starch material Plantic$^{\circledR}$. As well as being temperature dependent such materials are moisture dependent. Attempts are made in thermoforming processes to control the moisture level as, in particular, the pressure needed to deform the sheets is dependent on this. By contrast, the tests in [3], indicated that the final thickness distribution of the thermoformed structures is relatively insensitive to moisture change. For this reason we assumed in our model that the moisture content remains constant during the thermoforming process. The tests also suggested that there is little dependence on the rate of deformation, and that the permanent deformation and the stress-strain curve for uniaxial deformation indicates elastic-plastic deformation, see Fig. 1. Whilst many different constitutive models have been proposed for the modelling of polymer thermoforming, e.g. hyperelastic and finite viscoelastic, see [5] and [4], for the above reason our model assumed elastic-plastic deformation. In the application the deformation is moderately large and Fig. 1 suggests that most points are in the plastic region. Therefore our model, described in Section 3, assumes that the "elastic part" of the deformation is small compared to the "plastic part".

3 The mathematical model and the finite element implementation

We now give details of the mathematical model for the elasto-plastic sheet deformation and describe the explicit central difference scheme that is used in the LS-DYNA implementation.

3.1 The equations of motion

To describe the finite time-dependent deformation we introduce a number of terms used in continuum mechanics as follows.
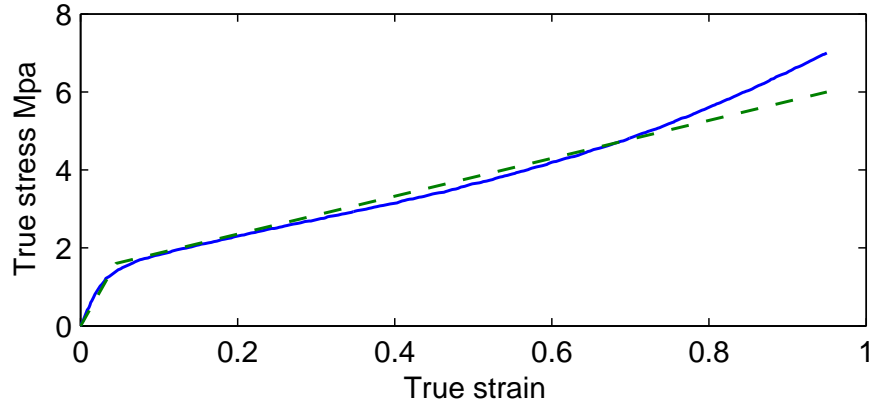
Fig. 1 Tensile test results at crosshead speed of 500 mm/min for the Plantic$^{\circledR}$ material equilibrated at initial 11.91% moisture content (solid line) and bilinear elasto-plastic fit (dashed line).

Let $\underline{x} = (x_i(t))$ denote the position of a point in the body (usually the current position), t denote time, $\underline{u} = (u_i(\underline{x}, t))$ denote the displacement from the starting state and $\underline{v} = (v_i(\underline{x}, t))$ denotes the velocity. As the sheet deforms it gets stressed and we let $\boldsymbol{\sigma} = (\sigma_{ij}(\underline{x}, t))$ denote the Cauchy stress. The equations of motion that the stresses satisfy are

$$\rho \ddot{x}_i = \left(\sum_{j=1}^{3} \frac{\partial \sigma_{ji}}{\partial x_j} \right) + \rho b_i, \quad i = 1, 2, 3, \quad \text{for any } t \in (0, T] \tag{1}$$

where ρ is the density and $\underline{b} = (b_i(\underline{x}, t))$ is the body force. To complete the description we now describe the elasto-plastic constitutive equations.

3.2 An elasto-plastic constitutive model

An elasto-plastic constitutive model involves expressing an appropriate time derivative of stress in terms of quantities involving the rate of deformation. These are typically used when the plastic part (p) of the deformation is large compared to the elastic part (e). Let

$$\mathbf{L} = \left(\frac{\partial v_i}{\partial x_j} \right), \quad \mathbf{D} = \frac{1}{2} \left(\mathbf{L} + \mathbf{L}^T \right) \quad \text{and} \quad \mathbf{W} = \frac{1}{2} \left(\mathbf{L} - \mathbf{L}^T \right),$$

where $\mathbf{L}$ is the velocity gradient, $\mathbf{D}$ is the rate of deformation tensor and $\mathbf{W}$ is the spin tensor. The elasto-plastic model involves writing

$$\mathbf{D} = \mathbf{D}^e + \mathbf{D}^p$$

where $\mathbf{D}^e$ and $\mathbf{D}^p$ are associated respectively with the elastic part and the plastic part of the deformation and $\mathbf{D}$ is an objective tensor.

An objective rate of stress is the Jaumann rate defined by

$$\overset{\triangledown}{\boldsymbol{\sigma}} = \dot{\boldsymbol{\sigma}} - \mathbf{W}\boldsymbol{\sigma} - \boldsymbol{\sigma}\mathbf{W}^T = \dot{\boldsymbol{\sigma}} - \mathbf{W}\boldsymbol{\sigma} + \boldsymbol{\sigma}\mathbf{W}. \tag{2}$$

The elasto-plastic constitutive model is such that

$$\overset{\triangledown}{\boldsymbol{\sigma}} = 2\mu\mathbf{D}^e + \lambda\mathrm{tr}(\mathbf{D}^e)\mathbf{I},$$

where λ and μ are Lamé constants and $\mathbf{I}$ is the identity tensor. To complete the description we need a yield function and a flow rule which govern how $\mathbf{D}^p$ evolves. We have here used the von Mises yield function and J_2 flow theory plasticity with isotropic linear hardening as it applies in the hypoelastic-plastic context. For details of how the elastic-plastic theory with infinitesimal strains maps to the large strain case with the use of the rates $\overset{\triangledown}{\boldsymbol{\sigma}}$ and $\mathbf{D}^p$ see [1, Sections 5.5 and 5.6]. With a specified value of the Poisson's ratio ($\nu = 0.3$ is used here), the slopes E and E^{tan} of the two dashed lines in Fig. 1 give all the parameters needed for this part of the model. The outcome is that we obtain a relation of the form

$$\overset{\triangledown}{\boldsymbol{\sigma}}_{ij} = \sum_{kl} C_{ijkl} D_{kl}, \tag{3}$$

where we have a different expression for C_{ijkl} depending on whether or not we are in the plastic region.

3.3 The explicit in time finite element method

For the numerical model we discretise in space and in time using finite elements to discretise the thin sheet in space and discrete times $0 = t^0 < t^1 < \cdots < t^n < \cdots$ at which we approximately satisfy the equations of motion. For the description we also need the mid-step-times which are defined by $t^{n+1/2} = (t^n + t^{n+1})/2$. The time steps involved are denoted by

$$\Delta t^{n+1/2} = t^{n+1} - t^n, \quad \Delta t^n = t^{n+1/2} - t^{n-1/2} = \frac{1}{2}\left(\Delta t^{n-1/2} + \Delta t^{n+1/2}\right).$$

In the following we use the notation $\underline{u}^{(n)}$, $\underline{v}^{(n)}$ and $\underline{a}^{(n)}$ to denote respectively all the nodal finite element displacement, velocity and acceleration parameters. Similarly $\underline{v}^{(n+1/2)}$ is the nodal velocity at time $t^{n+1/2}$. The finite element part involves taking the dot product of (1) with a finite element basis function and integrating over the region. This is further approximated by replacing the mass matrix by the "lumped mass matrix" which we denote by M. By construction M is a diagonal matrix. If $\underline{f}^{(n)}$ denotes all the nodal forces at

time t^n then

$$\underline{a}^{(n)} = M^{-1}\underline{f}^{(n)},$$

which just involves multiplying by a diagonal matrix. An outline of the explicit algorithm used in LS-DYNA is as follows.

For $n = 0, 1, 2, \ldots$

Determine the nodal forces $\underline{f}^{(n)}$ and the accelerations $\underline{a}^{(n)}$.

Get the velocities $\underline{v}^{(n+1/2)} = \underline{v}^{(n-1/2)} + \Delta t^n \underline{a}^{(n)}$.

Get the displacements $\underline{u}^{(n+1)} = \underline{u}^{(n)} + \Delta t^{n+1/2} \underline{v}^{n+1/2}$.

Update the geometry $\underline{x}^{(n+1)} = \underline{x}^{(n)} + \underline{u}^{(n+1)}$.

Update the stress quantities.

The update of the velocity is slightly different when $n = 0$. The update of stress quantities makes use of the constitutive model so that we have the stresses which contribute to the nodal force vector. With the velocities known at time $t^{n+1/2}$ we can obtain $\mathbf{L}$, $\mathbf{D}$ and $\mathbf{W}$ at time $t^{n+1/2}$ and by using (2) and (3) we can compute the Jaumann rate and $\dot{\boldsymbol{\sigma}}$ at time $t^{n+1/2}$ from which we define

$$\boldsymbol{\sigma}^{(n+1)} = \boldsymbol{\sigma}^{(n)} + \Delta t^{n+1/2} \dot{\boldsymbol{\sigma}}^{n+1/2}.$$

This updating is done at all the quadrature points used in each element.

As a final comment about the computational model, the LS-DYNA implementation involves frictional contact between the sheet and the mould although the parameters used are such that this is very close to total sticking.

4 Computational results

In Fig. 2 we show the cross-section of the axi-symmetric mould being used, together with the computed thickness ratio compared with that measured experimentally. The computational results were obtained using 1200 8-noded solid elements, with one element through the thickness. Given the limited amount of data available, and the uncertain accuracies of the data with respect to temperature and moisture content of the sheet in the thermoforming, the difference between the two curves is reasonably small.
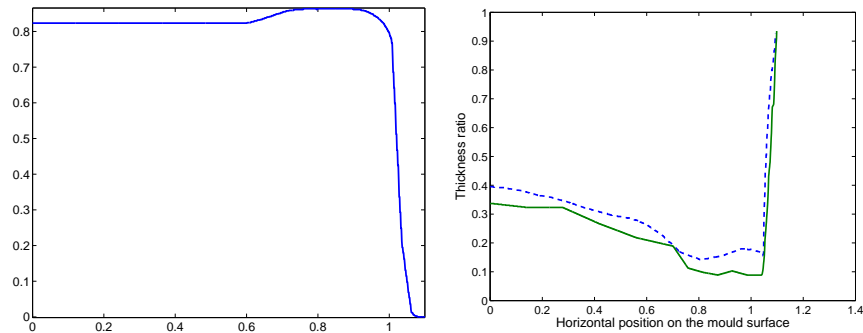
Fig. 2 Cross-section of the mould (left plot) and a comparison of the measured thickness ratio around the cross-section of the mould (solid line) with the results of the computational model (dashed line).

5 Conclusions and impact

This project has shown that computational modelling can be used successfully to predict wall thicknesses in thermoformed thermoplastic container structures. Reasonable accuracy was obtained using the assumptions of an elasto-plastic material model and effectively a total sticking sheet/mould-wall contact condition. All the results of the project were delivered to the company Plantic plc, at the time the world's largest manufacturer of starch based materials for packaging, who stated that they would provide technical information for their clients.

6 Acknowledgement

References

1. Belytschko, T., Liu, W., Moran, B.: Nonlinear finite elements for continua and structures. Wiley (2000)
2. Hallquist, J.O.: LS-DYNA Theory Manual (2006)
3. Szegda, D.: Experimental Investigation and Computational Modelling of the Thermoforming Process of Thermoplastic Starch. Ph.D. thesis, Brunel University (2009)
4. Szegda, D., Song, J., Warby, M.K., Whiteman, J.R.: Computational modelling of a thermoforming process for thermoplastic starch. AIP Conference Proceedings **908**(1), 35–48 (2007)
5. Warby, M., Whiteman, J., Jiang, W., Warwick, P., Wright, T.: Finite element simulation of thermoforming processes for polymer sheets. Mathematics and Computers in Simulation (61), 209–218 (2003)